Compact low-cost Arduino-based buoy for sea surface wave measurements

Conference Paper · November 2017

DOI: 10.1109/PIERS-FALL.2017.8293523

2 authors:

Yury Yurovsky
Marine Hydrophysical Institute
52 PUBLICATIONS **388** CITATIONS
SEE PROFILE

Vladimir Aleksandrovich Dulov
Marine Hydrophysical Institute
69 PUBLICATIONS **1,007** CITATIONS
SEE PROFILE

Compact Low-Cost Arduino-Based Buoy for Sea Surface Wave Measurements

Yu. Yu. Yurovsky[1] and **V. A. Dulov**[1]

[1]FSBSI Marine Hydrophysical Institute RAS, Russia

Abstract— This paper presents and describes a compact low-cost buoy for measurements of sea surface wave properties. Small micro-electro-mechanical (MEM) acceleration-gyroscope-magnetometer sensor data are stored onto internal buoy memory using open source Arduino hardware. The buoy has extremely simple internal architecture and small size because of deliberate disregard of autonomy and endurance, which is not necessary in short-term oceanographic measurements. Raw sensor data are processed after the measurements, so that various approaches can be validated and applied. Procedures for determining the buoy hull orientation and recovering wave signals are proposed. Possibilities in estimation of wave spectra and directional and spatial-temporal wave properties are demonstrated. From static ground calibration and field measurements in sea we have found, that internal MEM noise is insignificant for typical wave measurements. Low and high frequency disturbances caused by wind induced tilting, wave breaking kicks and resonant motions of the hull are discussed. A good consistence of estimated wave spectra with visual data and empirical spectral level model is demonstrated. Encouraging coincidence of elevation spectra calculated from independent acceleration, tilt and rotation signals is found.

1. INTRODUCTION

Retrieval of sea surface wave parameters from motions of floating bodies is a well known technique of *in situ* ocean wave measurements. Usually, the floating body is a tethered buoy having sensors of vertical acceleration (hull-fixed or stabilized) and orientation (based on magnetic field measurements) [1–3], or GPS-based velocity sensors [4, 5]. Combined sensor data allow to estimate basic properties of wave field: significant wave height, dominant wave direction and period, surface directional spectra. Such systems are fully autonomous and highly enduring, have tough massive hull, renewable power source, RF/GSM/satellite communication channel, etc. The listed abilities cause quite high price of the final product, however such a high degree of system reliability is not always necessary. For example, during scientific cruises the data are commonly collected over the nodes of evenly sampled grid (oceanographic stations). When number of such stations is large, small system deployment time and fast operation is preferred, while autonomy is redundant.

On the other hand, large size of traditional ocean buoys results in spatial filtering of waves shorter than buoy diameter (typically few meters). Although these waves have only small contribution to the total wave energy, they are responsible for transport processes at air-sea interface, and thus their investigation is also important [6–8].

Today there is a large number of ultra small and cheap acceleration/gyroscope/magnetometer (nine degrees of freedom, 9DOF) sensors that are widely used as an inertial measurement units in robotics engineering, entertainment, unmanned aerial vehicles navigation, virtual reality applications, etc. Such sensors can provide the same measurements as a hull-fixed accelerometers [9], while their total cost is few orders less than traditional oceanographic instruments. Small size of the sensor (several cubic millimeters) allows to use extremely small hulls with which short waves can be resolved (down to decimeter wave lengths).

In this paper we present a prototype of wave buoy built on the basis of micro-electro-mechanical (MEM) 9DOF sensor. Based on the preliminary test measurements carried out in field conditions we show that such sensors are suitable for oceanographic wave measurements. The problem of noise, which is the main drawback of cheap MEM inertial sensors, is also discussed.

2. INSTRUMENT DESIGN

The buoy is based on MEM 9DOF sensor (MPU9250) and Arduino controller. The raw sensor measurements are logged by Arduino Pro Mini board (3.3V, 8MHz), and stored onto micro-SD flash memory card (4GB, 4^{th} speed class). With a given parts, the resulting sampling frequency of the

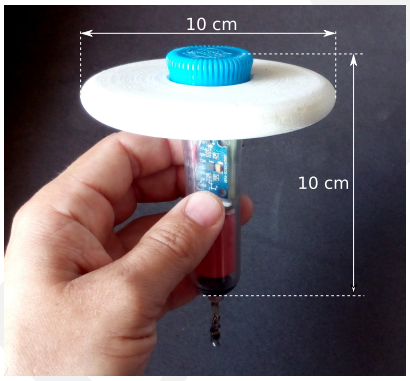

Part	Model
Controller	Arduino Pro Mini 3V, 8MHz
Sensor 9-DOF	MPU-9250
Memory card	MicroSD card 4GB with slot
Real time clock	DS3231
Battery	14250, Li-ion, 300 mAh
Battery charger	TP4056
Hull	PET bottle preform
Float	EPS packaging

Figure 1: Hand-held buoy prototype and its components.

system is about 160 Hz per one 16-bit channel. The number of channels is 11: 9 for 9DOF sensor, one is for sensor temperature, and one is for precise sample timing with microsecond resolution. The buoy is powered by 300 mAh Li-ion (14250 size) rechargeable battery. The battery USB charge controller is also built-in in the buoy for better usability. A self-powered real time clock is used for global time synchronization.

The hardware is assembled in cylindrical plastic waterproof hull (polyethylene bottle preform, 2.5 cm in diameter, length of 10 cm), which is inserted into discus shaped float made of expanded polystyrene. The float is 10 cm in diameter, 1 cm thick, but can be easily changed depending on measurement purposes (Fig. 1). Total weight of the buoy is 60 g.

The buoy hull is tied up to a spinning reel with a multi-filament 300 m length line. To use the buoy from non-moving (drifting or anchored) vessel one needs to throw it onto the sea surface and unwind the line so that the buoy drifts freely. Full battery charge is enough for about 10 hours of continuous operation, while one directional spectrum measurement usually can be done in 10-30 min, depending on wave peak period.

3. SENSOR DATA PROCESSING

3.1. Biases and Sensor Noises

The MEM sensor data have constant biases that should be subtracted for proper vector measurements. These biases were estimated from calibration records made with the buoy placed on a firm ground far from magnetic field distortions. The hull was rotated with 30 s interval to cover as many different orientations as possible. Considering only samples between rotations and assuming the measured vectors have constant magnitude (earth gravity for acceleration, zero rotation speed for gyroscope, and earth magnetic field for magnetometer) the biases for all nine signals of the 9DOF sensor were evaluated using least square method and then subtracted from measured signals. The same calibration records were also used for estimation of instrumental noise levels (see discussion below).

3.2. Buoy Orientation in Wave Field

Properly scaled sensor data provide vectors of acceleration, $\mathbf{a}$, rotation rate, $\mathbf{q}$, and magnetic field, $\mathbf{m}$, in the coordinates related to buoy hull, $\{x, y, z\}$. To know sea wave parameters, one needs to compute components of these vectors, $\mathbf{A}, \mathbf{Q}, \mathbf{M}$, and direction of the buoy vertical axis, $\mathbf{N}$, in earth-related coordinates $\{X, Y, Z\}$:

$$\mathbf{M} = \mathbf{R}\mathbf{m}, \quad (1)$$
$$\mathbf{A} = \mathbf{R}\mathbf{a}, \quad (2)$$
$$\mathbf{Q} = \mathbf{R}\mathbf{q}, \quad (3)$$
$$\mathbf{N} = \mathbf{R}\mathbf{n}, \quad (4)$$

where $\mathbf{R}$ is the rotation matrix, $\mathbf{n} = \{0, 0, 1\}^{\mathrm{T}}$. If pairs $\{\mathbf{m}, \mathbf{a}\}$ and $\{\mathbf{M}, \mathbf{A}\}$ are given, and crossproduct $\mathbf{L} = [\mathbf{MA}]$ is not equal to zero, a problem of determination of $\mathbf{R}$ has unique solution. Matrix elements R_{i1}, R_{i2}, R_{i3}, where $i = 1, 2, 3$, may be found by solving the following linear

equations:

$$M_i = R_{i1}m_1 + R_{i2}m_2 + R_{i3}m_3, \quad (5)$$
$$A_i = R_{i1}a_1 + R_{i2}a_2 + R_{i3}a_3, \quad (6)$$
$$L_i = R_{i1}l_1 + R_{i2}l_2 + R_{i3}l_3, \quad (7)$$

where $\mathbf{l} = [\mathbf{ma}]$. This is the case when the sensor is at rest and $\mathbf{A} = \mathbf{g}$, where $\mathbf{g} = \{0, 0, -9.8\}$ is the gravity acceleration. In case of sensor motion we have only two equations

$$|\mathbf{A}| = |\mathbf{a}|, \quad (8)$$
$$\mathbf{M} \cdot \mathbf{A} = \mathbf{m} \cdot \mathbf{a}, \quad (9)$$

and strict determination of all components of the A is unable. However if the sensor motion is induced by sea surface waves we can expect, in the frame of traditional linear wave theory, that $|\mathbf{A} - \mathbf{g}|/g = O(\epsilon)$, where $\epsilon = bk$ is the small value of wave steepness, b is the wave amplitude, and k is the wavenumber. Therefore, we propose an approximate method for estimating the elements of the rotation matrix $\mathbf{R}$.

We define the vector $\mathbf{A}$ so that the angle between $\mathbf{A}$ and $\mathbf{g}$ is minimal when the equations (8,9) are satisfied. In spherical coordinate system it reads

$$\mathbf{A} = a\{\cos\phi_M \sin\theta_A, \sin\phi_M \sin\theta_A, \cos\theta_A\}^{\mathrm{T}}, \quad (10)$$
$$\mathbf{M} = M\{\cos\phi_M \sin\theta_M, \sin\phi_M \sin\theta_M, \cos\theta_M\}^{\mathrm{T}}, \quad (11)$$
$$\theta_A = \theta_M + \arccos(\mathbf{a} \cdot \mathbf{m}/(am)). \quad (12)$$

Substituting (10) in (6), we obtain approximate elements of $\mathbf{R}$ for every time sample and recover the vectors $\mathbf{A}$, $\mathbf{N}$, and $\mathbf{Q}$ from equations (2-4). Notice, with this approach the important vertical acceleration A_z have an error of $O(g\epsilon^2)$. In small steepness approximation, wave slopes B and tilts T are

$$\frac{\partial\zeta}{\partial X} = B_X = -N_X, \quad (13)$$
$$\frac{\partial\zeta}{\partial Y} = B_Y = -N_Y, \quad (14)$$
$$T_X = \arctan(B_X), \quad (15)$$
$$T_Y = \arctan(B_Y), \quad (16)$$

where $\zeta(X, Y)$ is the sea surface elevation.

4. FIELD MEASUREMENTS

Preliminary validation of the designed buoy prototype was conducted in the Black Sea, during two days, about 1 km offshore at water depths around 30 m. *In situ* wind and wave measurements were taken from near-shore weather stations. On the first day (08-Jul-2017) the measurements were conducted under the gentle $3-5$ m/s north wind with swell coming from the north-west direction ("mixed sea" case, hereinafter). On the second day (22-Jul-2017), the fresh north wind with $6-8$ m/s speed was blowing for almost whole day, and no significant swell could be recognized visually ("wind sea" case, hereinafter).

The buoy vertical accelerations, rotation rates, and tilts, for the mixed sea case are shown in the Fig. 2. The signals are rather smooth. Variations of acceleration are much smaller than g, that is consistent with adopted approximation of small wave steepness. Small slopes of waves are also explicitly demonstrated in tilt time series. Slope oscillations dominate in rotation of the hull.

However some spikes in acceleration are sometimes evident (e.g. $t = 657$ s). From visual observation of the buoy, it was revealed that these events correspond to the moments when the buoy rapidly emerges from sea surface and then "squashes" back. These events happen on the crests of pre-breaking or breaking waves, where local acceleration is high enough to push the buoy out of the sea. Such spikes are quite rare and short, thus they do not significantly contributes to the mean values estimated from the signals. However, they keep important statistical information on wave breaking, which can be obtained using compact 9DOF sensors apart from wave spectrum estimation.

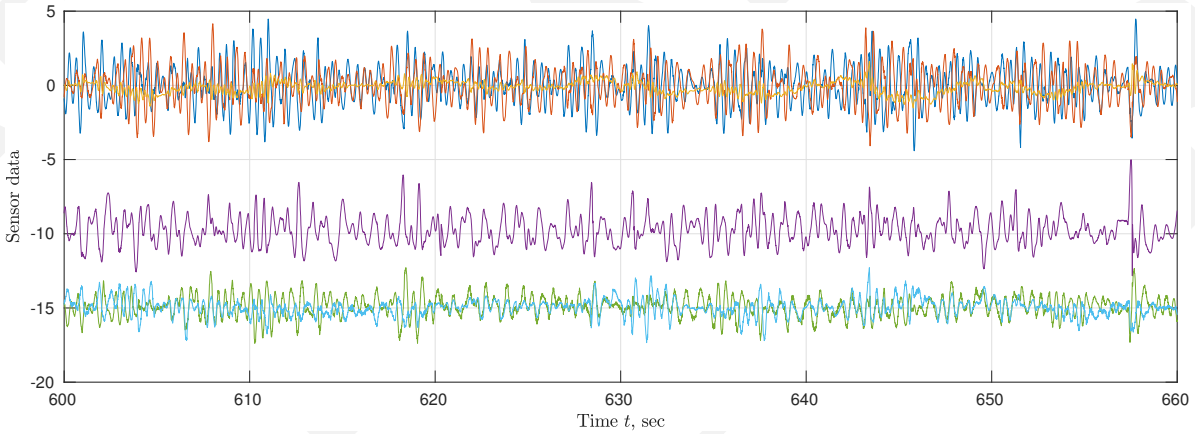

Figure 2: Fragment of time series on 08-Jul-2017. From top to bottom: gyroscope rotation rates in rad/s (blue – Q_x, red – Q_y, yellow – Q_z), vertical acceleration in m/s^2 (magenta – A_z), tilts in deg/10 (cyan – T_x, green – T_y).

4.1. Non-directional Elevation Spectra

We found the auto-spectrum of a signal $x(t)$ as $S_x(f) = \overline{|\mathrm{FFT}(x)|^2}$, where $\overline{(\ldots)}$ denotes averaging over consequent time segments of the record, and f is the frequency. Then spectrum of elevation spectrum S_ζ may be obtained with three independent manners from spectra of vertical acceleration, surface slopes, and horizontal rotation rates (see e.g. [3]):

$$S_{Az} = (2\pi f)^4 S_\zeta, \tag{17}$$

$$S_{Bx} + S_{By} = (k_x^2 + k_y^2) S_\zeta = k^2 S_\zeta, \tag{18}$$

$$S_{Qx} + S_{Qy} = (2\pi f)^2 (S_{Bx} + S_{By}) = (2\pi f)^2 k^2 S_\zeta, \tag{19}$$

where $k = \sqrt{k_x^2 + k_y^2}$ is the wave number.

Non-directional surface wave spectra are presented on Fig. 3 assuming linear dispersion relation of deep water surface waves, $(2\pi f)^2 = gk$. In frequency range from 0.2 Hz up to 1 Hz all three elevation spectra computed from eqs. (17-19) coincide within 95% confidence intervals. In the mixed sea case (Fig. 3a) two peaks are evident in line with visual observations. For the wind sea case (Fig. 3b), the spectrum is smooth and only one peak can be distinguished. As proposed by [10], levels of wind sea spectra lie between Toba's limits [11]: $S_1 = \alpha_1 g u_* (2\pi)^{-3} f^{-4}$ and $S_2 = \alpha_2 g u_* (2\pi)^{-3} f^{-4}$, where $\alpha_1 = 0.06$, $\alpha_2 = 0.11$, and u_* is the wind friction velocity. These limits are also shown on Fig. 3. We estimated friction velocity with the aerodynamic bulk formula $u_*^2 = C_\mathrm{D} U^2$, where the drag coefficient, C_D, and wind speed, U, are set to $C_\mathrm{D} = 1.5 \cdot 10^{-3}$, $U = 4$ m/s (mixed sea), and $U = 7$m/s (wind sea). Levels of wind sea spectra in Fig. 3b are consistent with Toba's limits while levels of swell spectra in Fig. 3a are beneath them. It is encouraging result because the raw signals were scaled using values from 9DOF sensor datasheet [12] without any additional "external" calibration.

4.2. Low frequency oscillations

In low frequency range, where f is below wind sea or swell peak, only accelerometer-derived spectrum exhibits a peak, while spectra computed from tilt and rotation rate has no visible (in log-log scale) peak. Such strong low frequency continuum is explained by the way which elevation spectra are derived from available data. The spectra of actually measured signals are multiplied by f^{-4} in (17), (18), or by f^{-6} in (19). If some white noise (flat spectrum) is present in the source data, this leads to a rapid growth, as fast as $f^{-4\ldots-6}$, of elevation spectra at low frequencies.

The first source of white noise in raw data is internal sensor noise. It was estimated from static calibration (see section 3.1) and transformed into noise-equivalent elevation spectra using eqs. (17)-(18) (Fig. 3, light blue and light red lines). Evidently this source is 3-5 orders weaker than the signal in valid wave motion frequency range $f < 4$ Hz, and can be ignored.

The second source low frequency noise is motion of the buoy due to the hull inclination by wind, hull interaction with holding line, wave breaking crests kicking the buoy, etc. This is typical

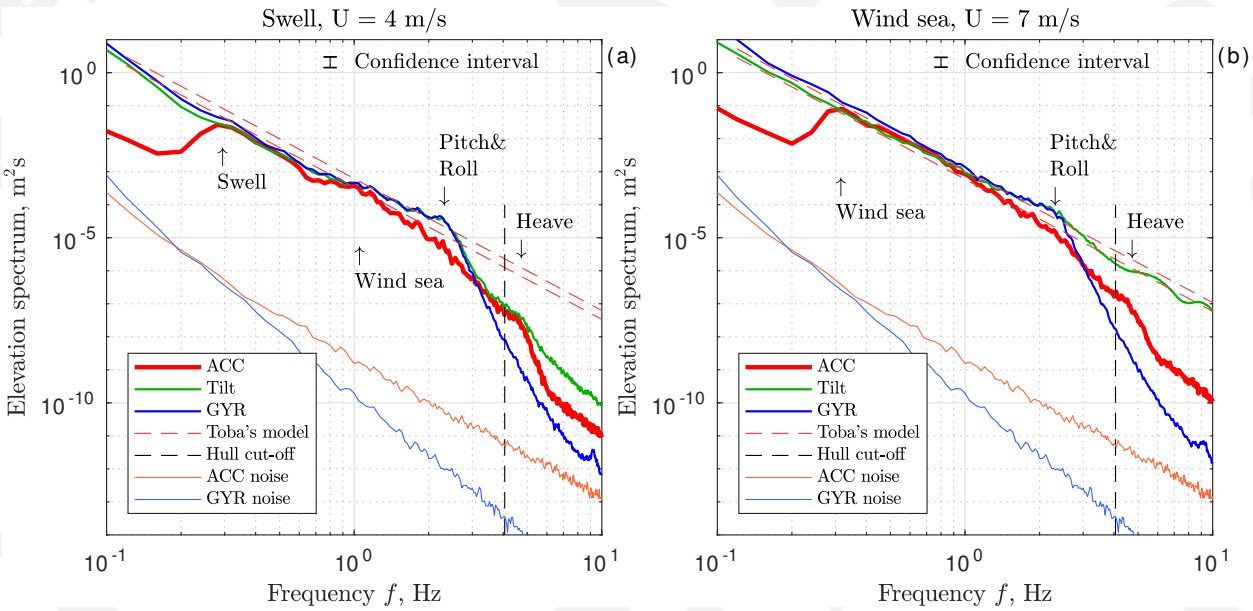

Figure 3: Non-directional elevation spectra for (a) swell (b) wind sea records estimated from accelerometer, gyroscope and tilt (combined accelerometer and magnetometer) data in comparison with Toba's [11] spectrum (red dashed lines) and noise-equivalent accelerometer (light red) and gyroscope (light blue) spectra. Vertical dashed line indicates wave frequency corresponding to wave-length equal to float diameter.

problem of buoy data processing [3], because these motions cannot be separated from "true" wave orbital motions, but can be minimized by specific hull shape and its holding configuration. The tilt of the buoy and its rotation rate are more affected by this source, while elevation spectra reconstructed from acceleration data demonstrate a well pronounced peak almost 2 orders higher than low frequency oscillation spectrum. Thus the elevation spectrum below the peak should be disregarded manually, or by some sophisticated high-pass filtering algorithm.

4.3. High frequency oscillations

The sensor cannot resolve waves whose length is shorter than some critical length determined by buoy size. The hull cut-off frequency for the float used in the experiment is $f_{\rm cr} = \sqrt{g/(2\pi d)} = 4$ Hz, where $d = 10$ cm is float diameter (Fig. 3, black vertical dashed lines). Some fading of the spectra is evident down to ≈ 2 Hz, indicating that waves longer than $\approx 4d$ are not filtered by the float, $f < 2$ Hz.

However, in the frequency range $1 < f < 2$ Hz there is a clear, $7 - 8$ times, disagreement between spectra derived from acceleration and that derived from rotation rate and tilts. This effect is explained by hull response to the excitation produced by waves. Similarly to a vessel, the buoy oscillations can be separated into pitch/roll (tilting) and heave (vertical) movements. The pitch and roll frequency is determined by metacentric height of the floating body, while the heave frequency depends on the body buoyancy, or, for discus shaped body, on the ratio of hull diameter and height. As revealed from the test measurements in small water tank (not shown here), our hull has resonant heave frequency at ≈ 4.5 Hz, which is higher than hull cut-off frequency. The pitch and roll movements, which frequency is ≈ 2.5 Hz, clearly explain the observed disagreement between the acceleration-derived and tilt-derived spectra. The effect of pitch, roll, and heave can be corrected by introducing response functions relating "true" and buoy measured spectra, like it is routinely done in large buoy data analysis [3]. On the other hand, if only long wave part of the spectra is interesting, $f < 1$ Hz for our particular hull, no compensation is necessary if such compact buoy configuration is used.

4.4. Directional Spectra and Spatial-Temporal Wave Properties

Simultaneous measurements of vertical acceleration and wave slopes in two orthogonal directions provide a basis for directional spectra estimation [1, 13, 14]. To demonstrate an ability of the 9DOF sensor to resolve wave directions we show on Fig.4 the directional spectra calculated using maximum entropy method [15]. The main peaks of the spectra are consistent with visually observed

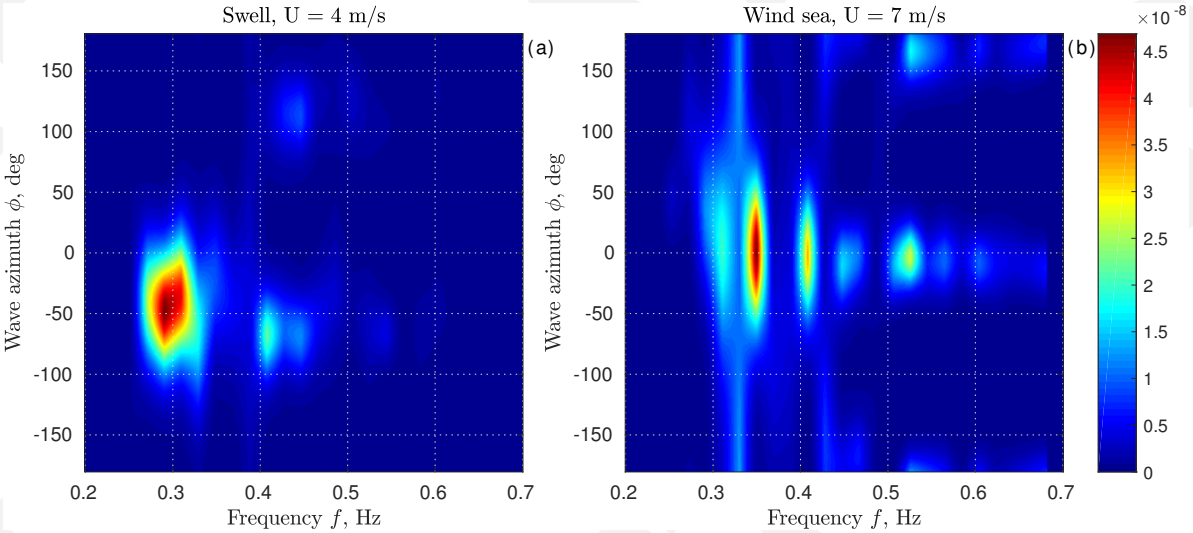

Figure 4: Directional elevation spectra for (a) mixed and (b) wind sea records computed using Maximum Entropy Method.

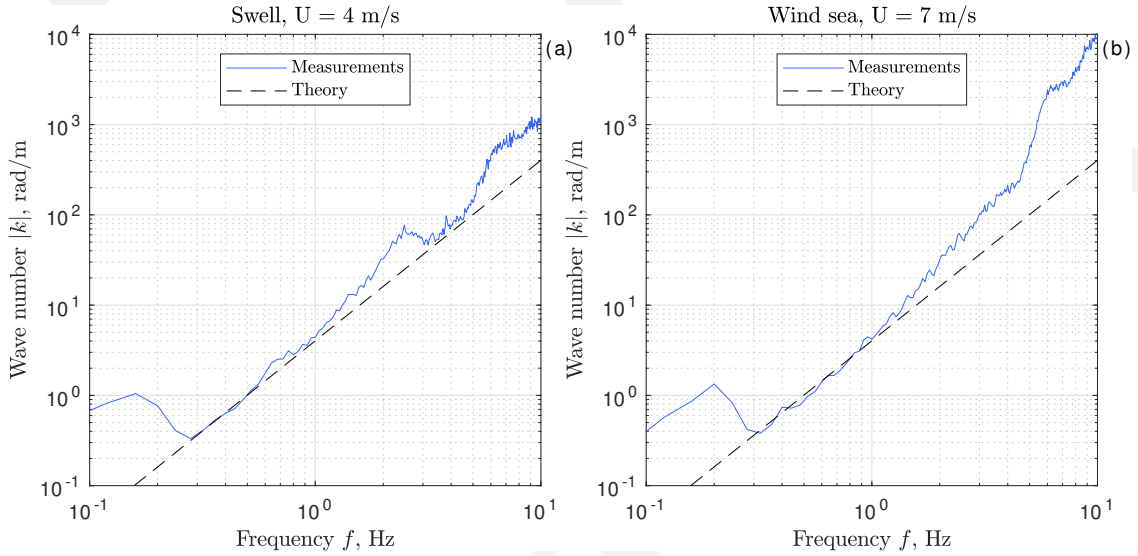

Figure 5: Dispersion relation for (a) swell and (b) wind sea records computed from estimated wave number and linear theory for surface gravity waves in the deep water.

wave directions.

Spatial-temporal wave properties are also accessible from simultaneous measurements of vertical acceleration and wave slopes [1, 13, 14], as it is follows from equations (17, 18). Dependencies of k on f calculated from these equations are shown on Fig.4. Linear dispersion relation for deep water gravity waves is also shown. Comparison of measured and theoretical dispersion curves shows their excellent agreement in the range of frequencies from spectral peak to hull cut-off frequency, $0.3 < f < 1$ Hz, indicating that approaches used in our analysis are reliable. Note, the drifting buoy measurement are not affected by Doppler shifts due to the currents, thus the dispersion relation remains unperturbed. Hence, the disagreement between measured and theoretical wave numbers can serve as a criterion for filtering out low and high frequency artifacts of the wave elevation spectra.

5. SUMMARY

On the basis of widespread MEM inertial motion sensor [12] that measures acceleration, rotation rate, and magnetic field, we have developed and present a buoy for measuring properties of sea

surface waves. The main features of the buoy are its uttermost simplicity, small size and low total costs (about $10). This is achieved by sacrificing its autonomy and endurance, which sometimes are redundant, e.g. in short-term oceanographic surveys.

The buoy is made of open source Arduino hardware, so it can be easily replicated and used in student trainings. Raw sensor data are stored onto internal memory card, so the processing performs at post-measurement stage. This allows for validation and improvement of various processing approaches and methods.

Small size of the buoy (10 cm diameter of the prototype, but can be further decreased) allows to resolve short waves on the sea surface, which are not available for traditional large wave buoys, but are interesting for oceanology scientists.

A significant drawback of cheap MEM sensors is their bad performance at low frequencies due to the internal noise. From the static noise estimation and two test field measurements carried out in real sea at gentle to fresh winds with and without swells we have found that internal noise can be tolerated under typical and even very calm sea states. However, a common for floating body measurements artifacts at low and high frequencies still occur due to the interaction of buoy with marine environment, but they can be disregarded or compensated using buoy hull response functions.

Using only the sensor datasheet [12] scaling parameters, without any additional calibration, we have found a very close and encouraging consistence of the measured and visually observed wave parameters, as well as good agreement with spectrum frequency fall-off, f^{-4}, and saturation level predicted by empirical Toba's model [11]. A possibility to estimate directional wave properties is also demonstrated. Further work will be dedicated to improvement of hull orientation reconstruction algorithms and more thorough inter-comparison with precise and independent *in situ* wave measurements.

ACKNOWLEDGMENT

The work was supported by State order of FSBSI Marine Hydrophysical Institute RAS under the project No. 0827-2014-0010 "Complex interdisciplinary research of oceanographic processes determining the functioning and evolution of the Black Sea and the Sea of Azov ecosystems on the basis of modern marine environment condition monitoring methods and grid technologies".

REFERENCES

1. M. S. Longuet-Higgins, D. E. Cartwright, and N. D. Smith, "Observations of the directional spectrum of sea waves using the motions of a floating buoy," in *Ocean Wave Spectra: Proceedings of a Conference, N. A. O. Sciences, Ed., Prentice-Hall*, pp. 111–132, 1963.
2. M. D. Earle and J. M. Bishop, *A practical guide to ocean wave measurement and analysis*. Marion, MA: Endeco, 1984.
3. M. D. Earle, R. Brown, D. J. Baker, and J. C. McCall, "Nondirectional and Directional Wave Data Analysis Procedures," NDBC Technical Document 96-01, Stennis Space Center, 1996.
4. G. Jeans, I. Bellamy, J. J. de Vries, and P. van Weert, "Sea trial of the new datawell gps directional waverider," in *Proceedings of the IEEE-OES Seventh Working Conference on Current Measurement Technology, 2003.*, pp. 145–147, March 2003.
5. T. H. C. Herbers, P. F. Jessen, T. T. Janssen, D. B. Colbert, and J. H. MacMahan, "Observing ocean surface waves with gps-tracked buoys," *Journal of Atmospheric and Oceanic Technology*, vol. 29, no. 7, pp. 944–959, 2012.
6. S. A. Kitaigorodskii and M. A. Donelan, *Wind-Wave Effects on Gas Transfer*, pp. 147–170. Dordrecht: Springer Netherlands, 1984.
7. E. J. Bock, T. Hara, N. M. Frew, and W. R. McGillis, "Relationship between air-sea gas transfer and short wind waves," *Journal of Geophysical Research: Oceans*, vol. 104, no. C11, pp. 25821–25831, 1999.
8. V. N. Kudryavtsev, V. K. Makin, and B. Chapron, "Coupled sea surface-atmosphere model: 2. spectrum of short wind waves," *Journal of Geophysical Research: Oceans*, vol. 104, no. C4, pp. 7625–7639, 1999.
9. M. Earle, K. Steele, and Y.-H. Hsu, "Wave Spectra Corrections for Measurements of Hull-Fixed Accelerometers," in *OCEANS 1984*, pp. 725–730, Sept 1984.
10. J. L. Hanson and O. M. Phillips, "Automated analysis of ocean surface directional wave spectra," *Journal of Atmospheric and Oceanic Technology*, vol. 18, no. 2, pp. 277–293, 2001.
11. Y. Toba and M. Koga, *A parameter describing overall conditions of wave breaking, whitecapping, sea-spray production and wind stress*, pp. 37–47. Reidel Publishing Company, 1986.

12. InvenSense Inc., "MPU-9250 Product Specification. Revision 1.1." Available at: https://www.invensense.com/wp-content/uploads/2015/02/PS-MPU-9250A-01-v1.1.pdf, 2016. Accessed 2010-09-30.
13. R. B. Long, "The statistical evaluation of directional spectrum estimates derived from pitch/roll buoy data," *Journal of Physical Oceanography*, vol. 10, no. 6, pp. 944–952, 1980.
14. H. E. Krogstad, "Conventional analysis of wave measurement arrays," in *Analysing the Directional Spectra of Ocean Waves* (K. Kahma, D. Hauser, H. E. S. Krogstad, S. Lehner, J. A. J. Monbaliu, and L. R. Wyatt, eds.), pp. 56–71, EUR 21367: EU COST Action 714, 2005.
15. A. Lygre and H. E. Krogstad, "Maximum Entropy Estimation of the Directional Distribution in Ocean Wave Spectra," *Journal of Physical Oceanography*, vol. 16, no. 12, pp. 2052–2060, 1986.